Mechanics of Jointed and Faulted Rock, Rossmanith (ed.) © 1990 Balkema, Rotterdam. ISBN 90 6191 155 9

Deformation of granite during triaxial friction tests

D.E. Moore, R. Summers & J.D. Byerlee
US Geological Survey, Menlo Park, Calif., USA

ABSTRACT: Cylinders of intact granite were loaded in triaxial testing equipment at room temperature until they failed in compression, and deformation was continued by sliding along the resulting breaks. At confining pressures between 40 and 120 MPa, the samples slid stably following the initial failure, and at confining pressures above 200 MPa they showed stick–slip motion. In the low–pressure, stably sliding samples, the shear was accommodated in zones within the main fault that are as much as 1.5 mm wide and that are characterized by a marked reduction in grain size, along with the formation of numerous synthetic Riedel shears and a fabric defined by deformed, elongate micas. In contrast, shear in the high–pressure, stick–slip samples was more highly localized along zones that are roughly 0.2 mm or less in width and that contain as many as four, 0.005 to 0.010 mm wide, subparallel shear bands consisting of extremely fine-grained gouge. Each shear band may represent a single episode of slip; thus, successive slip events in the stick–slip cycle occur as fresh breaks in the same part of the fault. The observed textural differences among the samples emphasize the correlation between stick slip and the localization of shear within fault zones. The patterns of deformation are very similar to those observed following friction experiments in which the samples contained a layer of artificial or natural gouge placed along a diagonal sawcut. This correspondence suggests that the deformation textures reflect the fundamental processes controlling the sliding behavior.

The overall configuration of the fault zones produced during the intact-rock experiments corresponds to the structure of many natural faults. In addition, repeated slip events along the nearly same path, similar to those occurring in the stick–slip samples, are also characteristic of faults such as the San Andreas of California.

1 INTRODUCTION.

Analysis of the deformation textures developed during triaxial friction experiments may be of fundamental importance in understanding the causes of stick–slip motion and, by inference, of earthquake processes in natural faults. We have examined many samples from friction experiments in which a layer of natural or artificial fault gouge was placed along a diagonal sawcut in a granite cylinder, so that shear was concentrated within the gouge layer (Moore, et al., 1986, 1988, 1989). The simplicity of a single, straight fault containing an initially uniform gouge zone facilitates petrographic study; however, most natural faults are not so simple. In order to obtain configurations that more closely approximate faults in nature but that nevertheless have been generated under controlled laboratory conditions, we have run a series of triaxial friction experiments using initially intact cylinders of granite. The cylinders were loaded until they failed in compression, and the loading was continued so that the samples slid along the generated breaks. The purposes of this study were: (1) to look for differences in the style of deformation between samples that slid stably and ones that showed stick–slip motion; and (2) to compare the textures with those produced in the samples containing a layer of gouge. The results of our preliminary textural examinations are reported in this paper.

2 PROCEDURES.

Cylinders of Westerly and Barre granite approximately 25 mm in diameter and 65 mm in length were used in the friction experiments. All of the experiments were run at room temperature, using either room-dry or fluid-saturated samples; no externally controlled pore pressure was applied. Axial compression rates were either 0.00635 or 0.000635 mm/sec, and confining pressures ranged between 40 and 620 MPa. Most of the friction experiments were run until the jackets failed; a few were terminated immediately following the initial failure of the granite, in order to separate the textural effects of the first break from those added as a result of subsequent shearing.

Thin sections of the faulted samples were examined; the sections were cut parallel to the long axis of the cylinder and perpendicular to the plane of the principal fault zone. The standard-sized sections contain the entire diameter but not the entire length of each granite cylinder. In most cases, the principal fault zone is completely contained in the thin section; the few exceptions are from samples in which the fault plane is oriented at a relatively low angle to the length of the granite cylinder. In order to obtain an overall picture of the fault and fracture patterns in the samples, deformation maps of the thin sections were constructed with the aid of a mechanical stage. Twenty-four faulted samples have been examined thus far.

3 RESULTS.

3.1 Strength and Sliding Stability

Plots of differential stress versus axial compression for representative experiments on Barre granite are presented in Figure 1; the rest of the strength data are contained in Summers and Byerlee (1977) and Moore et al. (1990). The results for the Westerly and Barre samples are comparable; in addition, the use of dry or fluid-saturated samples and of different axial loading rates had no obvious effects on strength or sliding behavior.

A sharp decrease in differential stress accompanies the failure point of the sample (Figure 1), which occurs after about 1.5 mm axial compression at low confining pressures and after about 4 mm at the highest confining

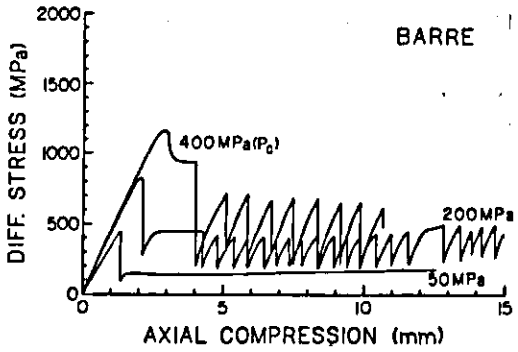

Fig. 1. Representative strength data for cylinders of intact Barre granite, illustrating the relationships among strength, sliding behavior, and confining pressure (Pc). The experiments plotted were run at room temperature on fluid-saturated samples, at an axial loading rate of 0.000635 mm/sec. The stress at initial failure and the subsequent frictional strength both increase with increasing confining pressure, and the sliding mode changes from stable to stick-slip.

pressures tested. The differential stress then increases slightly and subsequently levels off as shearing commences along the generated fault. At low confining pressures the sliding is stable, and at high pressures the sliding mode is stick-slip. Transitional behavior, that is, an early period of stable sliding followed principally by stick-slip motion, was observed in the 200 MPa Barre experiment (Figure 1) and in Westerly experiments run at confining pressures of 157 and 197 MPa (Summers and Byerlee, 1977). The differential stresses supported during shear increase with increasing confining pressure. A maximum of about 15 mm axial compression was attained during the experiments, which corresponds to roughly 17-18 mm offset along the principal fault zone.

3.2 Fractures and Faults

Maps displaying the major fractures developed in samples representative of the low-pressure, stable-slip experiments and of the high-pressure, stick-slip experiments are presented in Figures 2a and 3a, respectively. Similar maps for the remaining samples are contained in Moore et al. (1990). The two fault maps in Figures 2a and 3a display complex arrays of

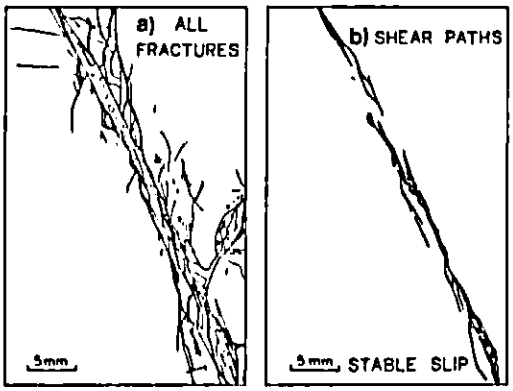

Fig. 2. Fault maps of a sample of Westerly granite that slid stably: a) map of all major fractures; b) those portions of the sample along which the shearing was concentrated. The experiment was run on a dry sample at 83 MPa confining pressure and 0.00635 mm/sec axial loading rate.

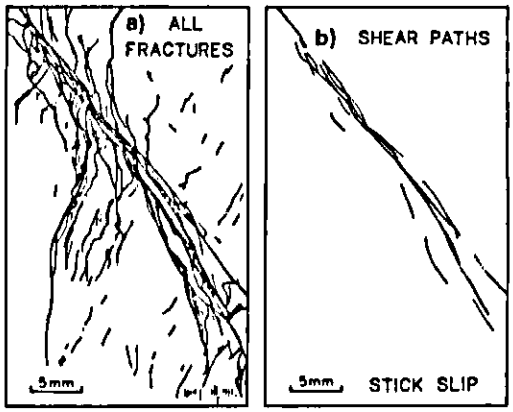

Fig. 3. Fault maps of a sample of Westerly granite that showed stick-slip motion: a) map of all major fractures; b) those portions of the sample along which the shearing was concentrated. The experiment was run on a dry sample at 485 MPa confining pressure and 0.000635 mm/sec axial loading rate.

fractures; the density of fracturing varies from sample to sample and is independent of both the confining pressure and the sliding behavior. In all samples, a principal fault zone of varying width crosses the cylinder. The average angle that the main fault zone makes with the axis of the granite cylinder tends to be higher in the samples that were run at higher confining pressures. For example, this angle is 26° for the 83 MPa sample (Figure 2a) and roughly 38° for the 485 MPa sample (Figure 3a). A similar relationship between fault orientation and confining pressure was observed by Paterson (1958).

The amount of fracturing decreases gradually with increasing distance from the main fault. The subsidiary fractures extend in all directions; the majority, however, have one of three principal orientations: parallel or perpendicular to the axis of the cylinder, or in a conjugate orientation to the main fault. Many of the fractures that intersect the main fault bend towards the trend of the fault near the point of contact; several good examples of this bending can be seen in Figure 3a. Given the great variation among the samples, no noticeable difference in fracture density was observed between samples for which the experiment was terminated at the initial failure and ones for which post-failure shear was permitted. In contrast, the outlines of the main fault zone are better defined after several millimeters of shear.

3.3 Distribution of Shear

Figures 2b and 3b depict the paths along which shear was concentrated during these two experiments. The textural criteria that were considered indicative of shear included the observable offset of minerals along fractures, a reduction in grain size, the development of a mineral fabric, and the formation of secondary shear bands. With only a few, very minor exceptions, the shearing during each experiment is centered on the main fault. The samples from experiments terminated at the initial failure exhibit only short, unconnected shear segments, whereas the samples that slid for several millimeters contain more or less continuous shear paths (Figures 2b and 3b). Apparent discontinuities may possibly connect outside the plane of the thin section or else they might have become connected if further shear had been possible.

The distribution of shear-related textures within a given fault is correlated with the sliding behavior. The locus of shear in the stably sliding sample (Figure 2b) is shown as a series of relatively wide zones, whereas the locus of shear in the stick-slip sample

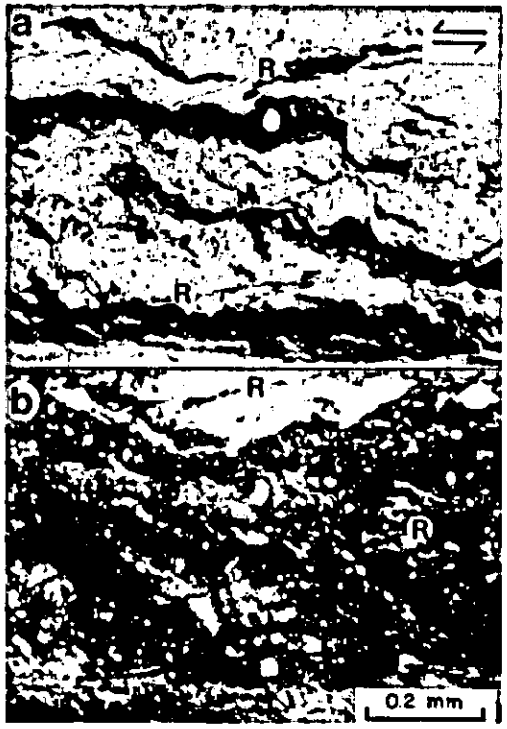

Fig. 4. Photomicrographs of part of the main slip path in a stably sliding sample: a) plane-polarized light, and b) crossed polarizers. Westerly granite, 83 MPa confining pressure; shear direction indicated by arrows. Best seen in a) are deformed biotites that are elongate from the lower right towards the upper left side of the photo. Best seen in b) is the pervasive reduction of grain size; slightly larger relict grains of quartz and feldspar are rounded. Also visible are faint traces of synthetic Riedel shears (R) that have the opposite orientation to the deformed biotites.

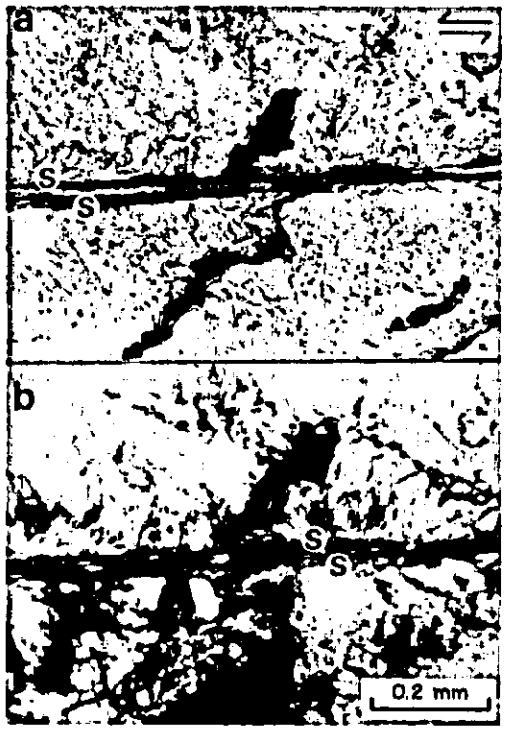

Fig. 5. Photomicrographs of part of the main slip path in a stick-slip sample: a) plane-polarized light and b) crossed polarizers. Barre granite, 400 MPa confining pressure; shear direction indicated by arrows. Two subparallel shear bands (S) consisting of extremely fine-grained gouge define a narrow shear zone that extends from left to right across the centers of the photos. Note the undeformed opaque mineral directly above the shear bands; quartz and feldspar crystals adjacent to the shear zone have been fractured but show no evidence of conversion to gouge. A biotite in the lower half of the photo has been squeezed out along a fracture.

(Figure 3b) is drawn as a set of interconnected lines. Such distinguishing features are also characteristic of the other stably sliding and stick-slip samples (Moore et al., 1990). These differences suggest that the shearing accompanying stick-slip motion is more highly localized than that accompanying stable slip.

Photomicrographs of portions of the shear path in a stably sliding and a stick-slip sample are presented in Figures 4 and 5, respectively. The photomicrographs illustrate that not only the width but also the textural elements visible in a given sheared area are functions of the sliding behavior. Shear is distributed across the entire field of view in Figure 4. The width of the shear path at this site is approximately 0.5 mm; the maximum measured width in the examined samples is about 1.5 mm. Fragments of quartz and feldspar in this zone show considerable cataclastic reduction in grain size to produce a relatively fine-grained gouge that has a dark appearance under crossed polarizers (Figure 4b). Relict larger grains of quartz and feldspar have acquired a rounded

outline as a result of wear. The relatively soft micas have been deformed into elongate shapes that define a rough mineral fabric (Figure 4a). Narrow, closely spaced, synthetic Riedel shears are faintly visible in both views in Figure 4; they are oriented at a low angle to the overall shear direction of the zone. Deformed biotite grains are slightly offset along the Riedel shears (Figure 4a), which imparts a stepped appearance to the biotites. The Riedel shears thus account for some portion – but not all – of the offset in these wide zones of stable slip.

The slip paths in stick–slip samples such as the one shown in Figure 5 are rarely more than 0.2 mm wide. These zones, in turn, consist of 1 to 4 subparallel shear bands, each one approximately 0.005 to 0.010 mm in width, that contain extremely fine–grained gouge. The very fine grain size gives the bands an isotropic appearance under crossed polarizers (Figure 5b); in plane light the bands vary in color from nearly colorless to dark brown, depending on the local mineral composition of the gouge. The shear zone in Figure 5 contains two shear bands, which are best distinguished in the plane–light view (Figure 5a). The granite adjacent to the shear bands has been fractured, probably during the initial failure of the sample, but it shows little evidence of cataclastic reduction in grain size. For example, an opaque grain located immediately above the shear zone in the photomicrograph is essentially undeformed.

4 DISCUSSION.

4.1 Fault Morphology and Comparison to Natural Faults

The fracturing and subsequent shearing of initially intact cylinders of granite in a triaxial machine yield samples showing complex and varying fracture patterns; however, the shearing is concentrated along a single main fault zone. The overall configuration of a main fault trace surrounded by a wide zone of fractured country rock is also characteristic of natural faults (e.g., Proctor et al., 1975; Flinn, 1977; Sibson, 1979; Chester and Logan, 1986). Shearing within the principal experimental faults is more highly localized in the samples that show stick–slip motion than in the ones showing stable slip. The stick–slip samples can therefore be described as displaying two levels of localization of shear: first, the formation of the main fault, and second, the restriction of shear to very narrow zones within the fault. This double localization has also been observed in natural faults (e.g., Chester and Logan, 1986), although in the natural case the physical features cannot be correlated to sliding behavior.

Each of the 0.005 to 0.010 mm–wide shear bands in the intact–rock samples showing stick–slip motion may represent a single episode of slip. In support of this possibility, the number of individual shear bands occurring together is always the same or less than the number of slip events in a given stick–slip experiment. This suggests that slip events can occur repeatedly along essentially the same path, but that the site of shear shifts from one place to another within the fault zone as a whole. The same distributions of shear along principal shear paths have been observed in natural faults such as the San Andreas and associated faults of California. For example, a given trench site across the San Andreas can yield evidence for several successive earthquakes (e.g., Sieh, 1978; Taylor et al., 1980), whose rupture traces follow nearly, but not exactly, the same path. Conversely, the active fault trace may shift position over time (e.g., Rogers, 1973), to produce a complex pattern of old and new traces similar to that sketched in Figure 3b.

4.2 Comparison with Gouge–Layer Experiments

A major purpose of this study was to compare the deformation textures developed in the samples from the intact–rock experiments with those from many previous experiments using a layer of artificial or natural fault gouge (Moore et al., 1986, 1988, 1989). Each sample in the earlier experiments (termed "gouge–layer experiments" in this paper) consisted of a granite cylinder through which a sawcut was made at a 30° angle to the cylinder axis. A layer of the gouge was placed along the sawcut surface, and during the friction experiments the shearing was concentrated within the relatively weak gouge layer. We have tested several different types of gouge, which nevertheless show comparable styles of deformation; for the present comparison, we will consider only those samples for which the gouge consisted of crushed and sieved Westerly granite.

Characteristic deformation textures developed in layers of the artificial granite gouge from stable– and stick–slip experiments are shown in Figures 6a and 6b, respectively. The initial particle size of both gouge layers is approximately that seen in Figure 6b. The gouge layer from the stable–slip experiment (Figure 6a) suffered a marked, overall reduction in grain size and a loss of angularity of the remaining larger grains as a result of the shearing. The gouge layer also displays a mineral fabric defined by deformed biotites, closely spaced Riedel shears, and shears that follow the boundaries between the gouge and the granite cylinder. In contrast, within the gouge layer from the stick–slip experiment (Figure 6b), the deformation has been localized to the Riedel and boundary shears only. Consequently, the gouge between shears is relatively undeformed, as seen by the numerous large and angular quartz and feldspar grains and the undeformed opaques in the areas between shears. The boundary shear zone in Figure 6b consists of only a single shear band; the boundary shear zones in several other samples, however, contain two, closely spaced shear bands and a few samples have three.

Despite the different starting configurations of the samples, the deformation textures that developed within the shear zones from the stable–slip experiments shown in Figures 4 and 6a are nearly identical. In addition, the shear bands from the stick–slip, intact–rock sample (Figure 5) are comparable to the individual shears developed in the gouge–layer sample that showed stick–slip motion (Figure 6b). The close textural correspondence between samples from corresponding gouge–layer and intact–rock experiments suggests that the same physical processes are operative whatever the initial sample configuration. Thus, the experimental conditions leading to a particular mode of sliding will also produce a particular style of deformation.

For the specific conditions of the intact–rock experiments, the sliding behavior was directly tied only to the confining pressure. Based on those samples and the ones shown in Figure 6, the confining pressure rather than the type of motion could potentially be correlated with the deformation textures. Comparison with other gouge–layer experiments, however, indicates that such a correlation may not be valid. Moore et al. (1986) conducted some

Fig. 6. Deformation textures developed in layers of artificial granite gouge during triaxial friction experiments at room temperature: a) stably sliding sample, 80 MPa confining pressure; crossed polarizers; b) stick–slip sample, 627 MPa confining pressure; plane polarized light. Shear directions are shown by arrows. The gouge of crushed Westerly granite was placed along a sawcut oriented at 30° to the axis of the containing granite cylinder. In both views, the width of the photo barely includes the entire width of the gouge layer. The initial particle size of both gouge layers was that shown in b). The stably sliding sample (a) therefore shows considerable grain–size reduction of quartz and feldspar, along with elongation of biotite and formation of synthetic Riedel shears (R). In the stick–slip sample (b) shearing is accommodated on the Riedel and boundary–parallel (B) shears, and the gouge between shears is essentially undeformed.

gouge–layer experiments using the artificial granite gouge at lower rates of axial loading than those tested in this study. The granite gouge showed a greater tendency to stick–slip

motion at the lowest rate of axial loading, and the stably sliding samples had a more pervasive deformation fabric than the stick-slip samples. Thus, a given type of sliding behavior in the granite gouge-layer experiments is correlated with a specific set of deformation textures, whatever the combination of experimental parameters producing it. To determine whether this conclusion is applicable to the intact-rock samples, they should be tested under a wider range of experimental conditions.

The deformation textures of stick-slip samples from the gouge-layer and intact-rock experiments do differ in one respect. In the gouge-layer experiments, two principal groups of shears occur in the stick-slip samples: 1) ones that are adjacent to the boundaries between the gouge layer and the rock cylinder, and 2) synthetic Riedel shears that crosscut the gouge layer. In the intact-rock samples that show stick-slip motion, the groups of shear bands appear to follow original fractures in the main fault. These fracture-following shears may be analogous to the boundary shears in the gouge-layer samples. The apparent absence of the Riedel-type shears from the stick-slip, intact-rock samples may possibly be a function of the narrow widths of the fractures along which shear occurs. Visible Riedel shears are found in the intact-rock samples that slide stably, because relatively wide zones of shear are generated in those samples. It is possible that the individual shear bands in the stick-slip samples may in turn have a submicroscopic fabric that includes Riedel shears as a fabric element. High-resolution studies should be conducted to study the internal fabric of the narrow shear bands.

5 SUMMARY AND CONCLUSIONS.

(1) The initial failure of granite cylinders under loading in a triaxial testing machine involves the formation of a complex array of fractures. Nevertheless, a main fault is discernible following the initial failure and becomes better defined after several millimeters of offset because of the concentration of shear along it. The angle between the main fault and the cylinder axis tends to increase with increasing confining pressure.

(2) The shear in samples that showed stable slip was accommodated in zones up to 1.5 mm in width within the main fault. These zones are characterized by a pervasive reduction in grain size, the development of a mineral fabric, and the formation of subsidiary synthetic Riedel shears that cross the zones of shear at low angles.

(3) Individual slip events in the samples that showed stick-slip motion were localized to shear bands within the main fault that are only 0.005 to 0.010 mm in width. The shear bands consist of highly comminuted fault gouge, and they generally occur in groups of 2 to 4 subparallel bands. This clustering suggests that slip events in the stick-slip cycle may occur repeatedly in essentially the same place on a fault. Conversely, the number of slip events in a given experiment is usually greater than the number of shear bands occurring together, indicating that movement may switch to other parts of the fault, perhaps as a result of strain hardening along the former slip paths. Both the clustering and the eventual shifting of slip paths also are characteristic of natural faults.

(4) The textural differences described between the intact-rock samples showing stable and stick-slip motion have also been observed in analogous samples containing a layer of simulated gouge placed along a sawcut surface. This correspondence suggests that the same fundamental controls on sliding behavior are operative, whatever the nature of the starting material.

REFERENCES

Chester, F.M., and Logan, J.M. 1986. Implications for mechanical properties of brittle faults from observations of the Punchbowl fault zone, California. Pure and Applied Geophysics 124: 79-106.

Flinn, D. 1977. Transcurrent faults and associated cataclasis in Shetland. Journal of the Geological Society of London 133: 231-248.

Moore, D.E., Summers, R., and Byerlee, J.D. 1986. The effects of sliding velocity on the frictional and physical properties of heated fault gouge. Pure and Applied Geophysics 124: 31-52.

Moore, D.E., Summers, R., and Byerlee, J.D. 1988. Relationship between textures and sliding motion of experimentally deformed fault gouge: Application to fault zone behavior. Proceedings of the 29th U.S. Symposium on Rock Mechanics: 103-110.

Moore, D.E., Summers, R., and Byerlee, J.D. 1989. Sliding behavior and deformation textures of heated illite gouge. Journal of Structural Geology 11: 329-342.

Moore, D.E., Summers, R., and Byerlee, J.D. 1990. Faults, fractures, and other deformation features produced during loading of granite in triaxial equipment. U.S. Geological Survey Open-File Report, in preparation.

Paterson, M.S. 1958. Experimental deformation and faulting in Wombeyan marble. Geological Society of America Bulletin 69: 465–476.

Proctor, R.J., Crook, R., Jr., McKeown, M.H., and Moresco, R.L. 1972. Relation of known faults to surface ruptures, 1971 San Fernando earthquake, southern California. Geological Society of America Bulletin 83: 1601–1618.

Rogers, T.H. 1973. Fault trace geometry within the San Andreas and Calaveras fault zones – A clue to the evolution of some transcurrent fault zones. Stanford University Publications in Geological Science 13: 251–258.

Rutter, E.H., Maddock, R.H., Hall, S.H., and White, S.H. 1986. Comparative microstructures of natural and experimentally produced clay-bearing fault gouges. Pure and Applied Geophysics 124: 3–30.

Sibson, R.H. 1979. Fault rocks and structure as indicators of shallow earthquake source processes. U.S. Geological Survey Open-File Report 79-1239: 276–304.

Sieh, K.E. 1978. Prehistoric large earthquakes produced by slip on the San Andreas fault at Pallett Creek, California. Journal of Geophysical Research 83: 3907-3939.

Summers, R., and Byerlee, J. 1977. Summary of results of frictional sliding studies, at confining pressures up to 6.98 kb, in selected rock materials. U.S. Geological Survey Open-File Report 77-142: 129 p.

Taylor, C.L., Cummings, J.C., and Ridley, A.P. 1980. Discontinuous en echelon faulting and ground warping, Portola Valley, California. California Division of Mines and Geology Special Report 140: 59–70.